A Novel Nuclear Factor-κB Gene Signature Is Differentially Expressed in Head and Neck Squamous Cell Carcinomas in Association with TP53 Status

Tin Lap Lee,[1,2] Xin Ping Yang,[1] Bin Yan,[1] Jay Friedman,[1] Praveen Duggal,[1] Lorena Bagain,[1] Gang Dong,[1] Ning T. Yeh,[1] Jie Wang,[2] Jian Zhou,[2] Abdel Elkahloun,[3] Carter Van Waes,[1] and Zhong Chen[1]

Abstract

Purpose: To determine if gene signatures differentially expressed in head and neck squamous cell carcinomas (HNSCC) are related to alterations in transcription factors nuclear factor-κB (NF-κB) and TP53 previously associated with decreased cell death, response to therapy, and worse prognosis.

Experimental Design: Unique gene signatures expressed by HNSCC lines were identified by cDNA microarray, principal components, and cluster analyses and validated by quantitative reverse transcription-PCR (RT-PCR) and *in situ* hybridization. Bioinformatic analysis of the promoters and ontogeny of these clustered genes was done. Expression of proteins encoded by genes of a putative NF-κB signature, NF-κB p65, and TP53 were examined in HNSCC tissue specimens by immunostaining. Predicted promoter binding and modulation of expression of candidate NF-κB genes and cell survival were evaluated by p65 chromatin immunoprecipitation (ChIP) and small interfering RNA (siRNA) knockdown.

Results: Two groups of HNSCC exhibiting distinct gene signatures were identified: cluster A enriched for histone genes, with a higher prevalence of TP53 promoter binding motifs; and cluster B enriched for injury response genes with NF-κB regulatory motifs. Coexpression of cluster B proteins was observed with strong NF-κB phospho-p65 and weak TP53 staining, and NF-κB phospho-p65 was inversely associated with TP53 ($P = 0.02$). Promoter binding of the NF-κB signature genes was confirmed by p65 ChIP, and down-modulation of their expression and cell death were induced by p65 siRNA.

Conclusion: NF-κB promotes expression of a novel NF-κB – related gene signature and cell survival in HNSCC that weakly express TP53, a subset previously associated with inactivated wild-type TP53, greater resistance to chemoradiotherapy, and worse prognosis.

Development and malignant progression of cancer includes multiple steps and mechanisms, which are rarely due to a defect of a single gene or pathway. The global gene expression profile of certain cancer types or subsets has been analyzed in depth by advanced microarray technology and bioinformatics, revealing the identification of gene programs or signatures contributing to the heterogeneous characteristics and malignant phenotypes among different cancer samples, even of the same pathologic classification (1–3). Such clustering of genes in distinctive signatures may result from common epigenetic or genetic changes or alterations affecting activation of common signal pathways and transcription factors that regulate programmed gene responses.

In head and neck squamous cell carcinomas (HNSCC), gene expression profiling has been used in an attempt to identify biomarker signatures for diagnosis (4), differential sensitivity to chemotherapy (5), risk of recurrence (6), survival (7), malignant phenotype (8), and metastasis (9). Although considerable variability in the composition of gene signatures was observed in these studies, the data provided evidence for subsets and heterogeneity within HNSCC, which are possibly related to differences in molecular pathogenesis and malignant potential. However, the mechanisms underlying the regulation of common and different gene programs contributing to the malignant phenotype in HNSCC have not been well defined.

In murine and human squamous cell carcinoma (SCC), we and others have independently shown altered activation of transcription factors TP53, nuclear factor-κB (NF-κB), activator protein 1 (AP-1), and signal transducers and activators of

Authors' Affiliations: [1]Tumor Biology Section, Head and Neck Surgery Branch, National Institute on Deafness and Other Communication Disorders, [2]Developmental Endocrinology Branch, National Institute of Child and Development, and [3]Microarray Unit, Cancer Genetics Branch, National Human Genome Research Institute, NIH, Bethesda, Maryland

Received 3/21/07; revised 5/20/07; accepted 5/25/07.

Grant support: National Institute on Deafness and Other Communication Disorders Intramural Project DC-00016.

The costs of publication of this article were defrayed in part by the payment of page charges. This article must therefore be hereby marked *advertisement* in accordance with 18 U.S.C. Section 1734 solely to indicate this fact.

Note: Supplementary data for this article are available at Clinical Cancer Research Online (http://clincancerres.aacrjournals.org/).

C. Van Waes and Z. Chen contributed equally as senior authors. T.L. Lee and X.P. Yang contributed equally as first authors.

Current address for T.L. Lee: Laboratory of Clinical Genomics, National Institute of Child Health and Human Development, NIH, Bethesda, MD.

Requests for reprints: Zhong Chen or Carter Van Waes, Head and Neck Surgery Branch, National Institute on Deafness and Other Communication Disorders/NIH, 10/5D55, MSC-1419, Bethesda, MD 20892-1419. Phone: 301-435-2073; Fax: 301-402-1140; E-mail: chenz@nidcd.nih.gov or vanwaesc@nidcd.nih.gov.

doi:10.1158/1078-0432.CCR-07-0670

transcription 3 (STAT3) and their functional roles in the expression of individual genes and phenotypic characteristics. Dysfunction of *TP53* in HNSCC frequently results from mutation and is often associated with aberrant overexpression and immunostaining for TP53 protein, which occurs in ~50% of HNSCC (10, 11). Inactivation of wild-type (wt) TP53 with weak expression and immunostaining is observed in most others, resulting from the inactivation of the p14ARF/p16INK4a locus regulating *TP53* activation, or rapid protein degradation, from human papillomavirus (HPV) E6 gene expression (10, 12, 13). The mutation or loss of expression of *TP53* has been implicated in a decrease in programmed cell death (14, 15). Interestingly, HNSCC retaining wt *TP53* genotype but weakly expressing TP53 protein are associated with greater resistance to chemotherapy and/or radiation than those expressing mutant TP53 in clinical trials and studies *in vitro* (16, 17). However, the molecular basis for this observation and possible relationship to expression of various other genes previously associated with differences in malignant potential is not fully understood.

We discovered that NF-κB is constitutively activated in HNSCC and have shown that the activation of NF-κB/RelA (p50/p65) is one of the important factors controlling the expression of multiple genes that regulate cellular proliferation (*Cyclin D1*), apoptosis (*cIAP1*, *Bcl-xL*), angiogenesis (*IL-8*), immune and proinflammatory responses (*IL-6*), and therapeutic resistance of HNSCC and murine SCC (18–25). Variable increase in nuclear localization of NF-κB is also observed in tumors of ~85% of patients with HNSCC, with stronger immunostaining associated with worst prognosis (26). NF-κB has become widely implicated in the pathogenesis of other diseases and cancers (27–32). However, the potential relationship between NF-κB regulated gene expression and TP53 status in HNSCC has not been previously reported.

Here, we examined global expression profile data for human HNSCC and primary keratinocyte lines by cDNA microarray and identified two subgroups of HNSCC cell lines with distinct gene expression signatures. Interestingly, bioinformatic analysis revealed that the subgrouping of the HNSCC cells was associated with differences in expression of known and putative NF-κB target genes. Known NF-κB target genes involved in cell proliferation, survival, and angiogenesis, such as *IL-6*, *IL-8*, and *c-IAP1*, were most strongly expressed in HNSCC cell lines with wt TP53 and tumor specimens with minimal or weak TP53 protein expression. Nuclear staining of the activated phospho-Ser^{536} form of p65 was inversely related to TP53 staining. These findings provide evidence that NF-κB activation and TP53 status are important determinants of distinct patterns of gene expression and linked in HNSCC. NF-κB and related genes could be important in the pathogenicity, resistance to chemoradiotherapy, and poor prognosis previously associated with the subset of HNSCC with impaired TP53 expression or function.

Materials and Methods

Cell lines and cell culture. Ten UM-SCC cell lines were from the University of Michigan series (Dr. T.E. Carey, University of Michigan, Ann Arbor, MI; Supplementary Methods and Supplementary Table S1). The cell lines were maintained in EMEM supplemented with 10% fetal bovine serum and penicillin/streptomycin. The *TP53* mutation and expression status of UM-SCC cells lines were determined by bidirectional genomic sequencing of the exons 4–9 of *TP53* and confirmed with immunocytochemistry using antibody of DO-1 (Supplementary Fig. S1; ref. 33). No mutation was detected in exons examined in four cell lines, UM-SCC 1, 6, 9, and 11A, and missense mutation of *TP53* was detected in five cell lines, UM-SCC 5, 22A, 22B, 38, and 46 (Supplementary Fig. S1; ref. 33). A *TP53* mutation was detected in UM-SCC 11B cells; however, immunocytostaining for TP53 protein indicated a weaker heterogeneous pattern of TP53 expression in UM-SCC 11B. The results of *TP53* sequence analysis in UM-SCC 1, 5, 6, 11B, and 46 cells are consistent with those independently determined and previously reported by Bradford et al. (16). Human primary normal keratinocytes (HKC) derived from adult skin were obtained from Cascade Biologics Inc. and were maintained in keratinocyte serum-free medium 154CF containing 0.08 mmol/L Ca^{2+} with human keratinocyte growth supplements (HKGS). All HKC were used within five passages.

cDNA microarray and data analysis. Detailed methods for cDNA microarray and data analyses are recently published (34) and described in Supplementary Methods. Briefly, 50 to 100 μg of total RNA isolated using TRIzol reagent (Invitrogen) was reverse transcribed to fluorescence-labeled target cDNA with Cy3 or Cy5-dUTP (Amersham Pharmacia Biotech Inc.). Labeled targets were hybridized to 24K human array chips (National Human Genome Research Institute). Fluorescence images were captured by GenePix 4000 microarray scanner (Axon Instruments) and analyzed using the ArraySuite 2.1 extensions in IPLab program (Scanalytics, Inc.; ref. 35). Data analyses includes PCA analysis (Partek Pro 5.1, Partek Inc.), hierarchical clustering (36), Java Treeview (37), BRB-Array Tools,[4] Gene Ontology, DAVID (Database for Annotation, Visualization, and Integrated Discovery, National Institute of Allergy and Infectious Diseases, NIH, Bethesda, MD), LocusLink [National Center for Biotechnology Information, NIH]. A mixed-model–based *F* test was used to analyze differential gene expression between different clusters (38, 39). This statistical model was carried out by using SAS 9.1 program (SAS Institute Inc.). $P < 0.05$ was designated as significant difference.

Real-time reverse transcription-PCR and* in situ *hybridization. Real-time reverse transcription-PCR (RT-PCR) and *in situ* hybridization for validation of microarray gene expression were done using standard methods as described in Supplementary Methods.

Bioinformatic prediction of promoter transcription factor binding motifs. To detect transcription factor binding sites in the promoter region on selected gene clusters, promoter analysis was done by Genomatix software suite 3.4.1 using the default matrix index. The proximal promoter sequences of each gene have, on average, ~600 bp in length, located from ~-500 bp to +100 bp of the transcription start site. We used all NF-κB binding matrices, including p65, p50, and c-Rel. The binding site of TP53 included the 20- to 21-bp decamer sequence. The predicted binding sites of AP-1 and STAT included the binding motifs for all the transcription factor members in the families. The statistical significance was examined by χ^2 analysis.

Immunohistochemical analysis of HNSCC tissue arrays and specimens, chromatin immunoprecipitation assay. Detailed information is described in Supplementary Methods.

Transient transfection with p65 RNAi plasmid or oligo nucleotides. Transient transfection of p65 RNAi plasmid (Imgenex) or p65 RNAi (SMARTpool, Dharmacom) was carried out using LipofectAMINE 2000 reagents according to manufacturer's protocol (Invitrogen). The transfection efficiency of plasmids was evaluated by RSV-LacZ construct (American Type Culture Collection). The effectiveness of p65 RNAi was confirmed in UM-SCC cells with high constitutive p65 activity by transient transfection, where p65 gene and protein expression and binding activity were decreased by more than 70% at 72 h after transfection (19).

[4] http://linus.nci.nih.gov/BRB-ArrayTools.html

Luciferase reporter gene assay. UM-SCC 1 and 9 cells were cotransfected with 5× NF-κB luciferase reporter plasmid (Clontech) and internal control plasmid RSV-LacZ using LipofectAMINE 2000 transfection reagent (Invitrogen) for 4 h in triplicates. Cell lysates were collected 48 h after transfection, and the luciferase activity was measured using Dual Light Reporter Gene assay (Tropix) on Monolight 2010 luminometer (Analytical Luminescence Laboratory). β-Galactosidase activities were determined to verify the reproducibility of each transfection experiment, and luciferase activities were normalized with β-galactosidase activity in each transfection experiment.

Results

Gene expression profiling with principal components analysis and unsupervised hierarchical cluster analysis. Ten UM-SCC cell lines were used for gene expression profiling by cDNA microarray (Supplementary Table S1). Many of the molecular alterations and biological characteristics of these cell lines have been confirmed to reflect those identified in HNSCC tumors from patients in laboratory and clinical studies, including the role of activation of epidermal growth factor receptor (EGFR), interleukin 1 (IL-1) and IL-6 signal transduction pathways; altered activation of transcription factors TP53, NF-κB, AP-1, and STAT3; expression of cytokines and other genes; and radiation and chemosensitivity (5, 16, 20, 21, 23, 40–44). Nonmalignant human keratinocytes (HKC) used for comparison were from four donors, and these cells were harvested in the exponential growth phase to minimize the effects of differentiation. Gene expression profiles were obtained using a 24K cDNA microarray (National Human Genome Research Institute, NIH), and the expression of 9,273 of 12,270 evaluable known genes were submitted for principal components analysis (PCA; Fig. 1A). PCA classified the UM-SCC cell lines and HKC into two groups by component 1 on the *X*-axis and the UM-SCC lines into two subgroups by component 2 on the *Y*-axis (SCC_sub_1 and SCC_sub_2).

To investigate the critical genes contributing to the subgroups of cell lines, 942 genes were initially identified using at least a 2-fold difference in average expression ratio between UM-SCC and HKC (Student's *t* test, $P < 0.01$; refs. 45–48). This was followed by an additional global permutation test that excludes genes differing significantly due to chance alone. Genes that showed significant differences ($P < 0.001$) after 2,000 permutations were classified as differentially expressed genes. Using unsupervised hierarchical cluster analysis, three major hierarchical branches were identified, which included the group of four HKCs and two UM-SCC groups (Fig. 1B), each comprising the same cell lines that were segregated into subgroups by PCA. Of the 942 genes, 385 and 557 genes showed either increased or decreased expression, respectively, in UM-SCC cells when compared with that in HKC (Fig. 1B). The selected list of genes that are significantly up- or down-regulated in HNSCC cell lines are presented in Supplementary Table S2A and B. Two distinct gene expression patterns associated with each of the two subgroups of UM-SCC cells were observed and designated as cluster A (up-regulated in subgroup-1, including UM-SCC 5, 22A, 22B, 38, and 46) and cluster B (up-regulated in subgroup-2, including UM-SCC1, 6, 9, 11A, and 11B). Ontology annotation of the clusters A and B genes is presented in Supplementary Table S3. We used a mixed-model–based *F* test to examine statistical difference of gene expression among HKC and the subgroups of UM-SCC

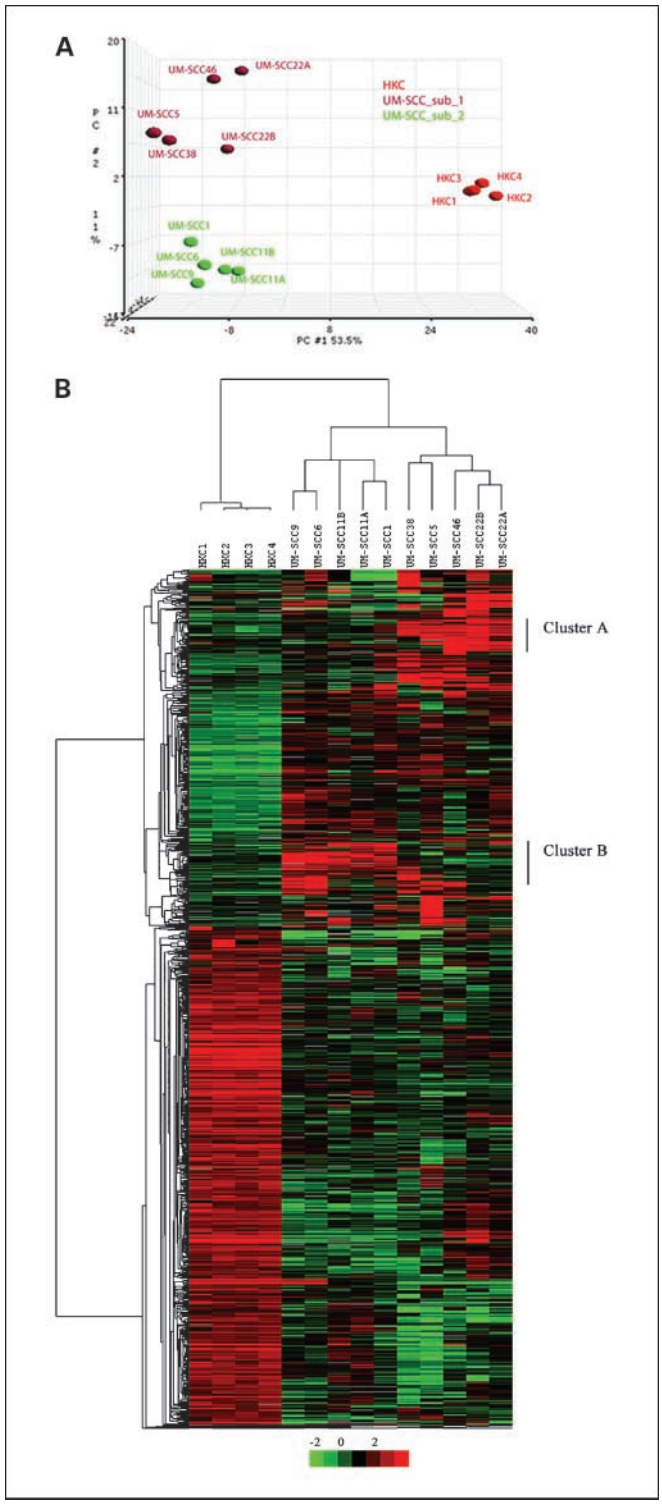

Fig. 1. Gene expression profiles clustered UM-SCC and HKC cells using PCA and unsupervised cluster analysis. *A,* three-dimensional presentation of PCA of three major clustered sample groups. Each dot represents one sample calculated based on values of all 9,273 genes, whereas the percentage of variances represented were indicated in three axes. The distance in space between the colored boxes represents the degree of relatedness between the cell lines. *B,* hierarchical clustering dendrogram was established based on 942 genes identified to have greater than or equal to 2-fold differences between the average values of 10 UM-SCC cell lines and that of 4 primary human keratinocyte (HKC) clones. The heat map was scaled using $\log_2$-converted expression ratio of subjects (normal and tumor) to the universal reference for particular gene. Distinct cluster *A* and *B* gene expression patterns were denoted.

cells overexpressing clusters A and B genes in Fig. 1B. In cells expressing cluster A genes, a difference in expression with statistical significance with $P < 0.0001$ was observed when compared with expression in UM-SCC with the cluster B pattern or with HKC. In cells expressing cluster B genes, a difference in expression with $P < 0.001$ was obtained when compared with UM-SCC cells expressing cluster A or with HKC.

We noted that the segregation of UM-SCC lines into two equivalent subgroups approximates the frequencies of ~50% each for TP53 inactivation and mutation reported for HNSCC (49, 50). *TP53* gene mutation and protein expression in these cell lines were examined (Supplementary Fig. S1; ref. 33).[4] Briefly, missense mutations in *TP53* were detected in 6 out of 10 cell lines, and TP53 nuclear protein expression was detected by immunostaining in 5/6 of these UM-SCC cell lines with mutant TP53 status (Supplementary Fig. S1B). Thus, in most cases, the subgrouping of UM-SCC by gene expression profiling were associated with their TP53 status, with the exception of UM-SCC 11B line, which exhibited a more heterogeneous pattern of TP53 immunostaining, and clustered with wt TP53 UM-SCC, including UM-SCC 11A derived from the same patient. Analysis of the expression and function of wt and mutation TP53 in these UM-SCC lines are under way to determine the basis for the association of cluster A and B gene expression with TP53 status, and for exceptions, such as UM-SCC-11B.

Validation of gene expression by real-time RT-PCR and* in situ *hybridization. A set of differentially expressed genes was further validated by real-time RT-PCR, including eight up-regulated and four down-regulated genes in UM-SCC (Fig. 2A). Concordant data were observed between microarray and real-time RT-PCR, indicating the reliability of the microarray analyses. Notably, the expression of cluster B genes *IL-6*, *IL-8*, *c-IAP1*, and *YAP1* were increased mainly in subgroup 2 of UM-SCC lines. Conversely, expression of cluster A gene *HIST1H2BN* was increased mainly in subgroup 1 of UM-SCC lines. Other up-regulated genes, such as the antiapoptotic genes *BAG2*, *TRAF2*, and *CCNB2*, as well as the down-regulated genes *IL-1R2*, *CDKN1A*, *CCNG1*, and *CSF2*, were detected in most of the UM-SCC lines by both methods (Fig. 2A).

We further validated four up-regulated genes in eight human HNSCC tissues and two matched normal mucosa tissues by *in situ* hybridization. We selected *CCND1* and *PCNA*, which have previously been reported to be overexpressed in SCC (6, 18, 22, 51, 52), and *BAG2* and *CCNB2*, which have been less studied (Fig. 2B). In each experiment, we included tumor tissues from UM-SCC 11A xenograft using antisense probe as a positive control (a), and sense probe as the negative control (b). On the top left, the *BAG2* antisense probe strongly hybridized to UM-SCC 11A xenograft tumors (*white arrows*, a) and patient HNSCC tumor tissues (*white arrows*, c), but not on the matched normal mucosa tissues (e). Sense control probes did not hybridize to any of the tissues (b, d, and f). Similar hybridization patterns were observed when using *PCNA*, *CCND1*, and *CCNB2* probes (Fig. 2B, remaining graphs). In d for *CCND1* (*top right*) and *CCNB2* (*bottom right*), we used antisense probes in a HNSCC tumor tissue with adjacent mucosa. Most of the hybridization signals were found in tumors but not normal mucosa (*white arrows*). Our data indicated that the expressions of these genes identified from microarray studies in cell lines are similarly expressed in human HNSCC tissues.

Increased prevalence of TP53 and NF-κB binding motifs within the proximal promoter regions of clustered genes. We hypothesized that the differences in clustered gene expression observed could be related to transcription factors previously shown to be altered in HNSCC, such as TP53, NF-κB, AP-1, and STAT3. To test this hypothesis, the proximal promoter sequences of the genes in both clusters were extracted and analyzed using algorithms by Genomatix Software Suite 3.4.1, which evaluates the average optimal length of ~600 bp, from -500 to +100 bp of transcription start sites (Genomatix; Supplementary Table S3). The presence of putative recognition sites for the four transcription factors using this algorithm are summarized adjacent to the clusters in Fig. 3A and B, and the frequency of the predicted promoter binding sites were calculated and presented in Fig. 3C. In cluster A, binding sites for TP53 were present at increased frequency (9/17, 53%), when compared with genes in cluster B (6/27, 22%). Conversely, NF-κB binding sites (including all NF-κB family members) are highly represented in cluster B (20/27, 74%) when compared with cluster A genes. Interestingly, when we further analyzed the preferred binding motifs for different NF-κB subunits, a predominance of p65 binding motifs were observed in the promoters of cluster B genes, in contrast to the prevalence of p50 and c-REL binding motifs present in the promoters of cluster A genes with putative NF-κB binding sites.[5] Significant differences in the prevalence of TP53 and NF-κB p65 binding sites were detected between clusters A and B (Fig. 3C, χ^2, $P < 0.05$). Consistent with promoter analysis, the genes in the cluster B include several genes previously shown to be regulated by NF-κB, such as *IL-6*, *IL-8*, *c-IAP1*, and *ICAM1* (19, 23, 53–55). Higher frequencies of the binding motifs for AP-1 and STAT were also represented in cluster B genes, but did not reach statistical significance (Fig. 3C). The detailed analyses of predicted transcription factor binding sites of the clusters A and B from the up-regulated genes in UM-SCC cells are presented in Supplementary Table S3.

Immunostaining for putative NF-κB regulated proteins, NF-κB, and TP53 in HNSCC tissues. We recently confirmed that the UM-SCC cells in the panel with wt TP53 genotype stain weakly with anti-TP53 antibody DO-1 when compared with those with mutation TP53 (33). To explore the potential relevance of the apparent relationship between NF-κB regulated gene expression and TP53 status in UM-SCC cell lines to HNSCC tumors, we examined if a relationship exists between NF-κB p65 and TP53 staining patterns in fixed tumor tissues from patients with HNSCC of upper aerodigestive tract mucosal sites (oral cavity, pharynx, and larynx). Upon analysis of tissue microarrays of HNSCC and normal oral mucosa, 10 of 20 samples (50%) showed strong TP53 staining, and increased NF-κB p65 staining was observed in 14/20 (70%) of tumor samples, compared with normal mucosa (Fig. 4A). A total of 6/20 (30%) of the samples showed strong NF-κB staining with no detectable TP53 staining (*top left*); 8/20 (40%) showed some staining for both NF-κB p65 and TP53 (*bottom left*); 3/20 (15%) cases showed strong TP53 staining with no NF-κB p65 staining (*top right*); and three tumors (3/20, 15%) showed negative staining for both antibodies (data not shown). No or minimal

[5] Bin Yan, unpublished observation.

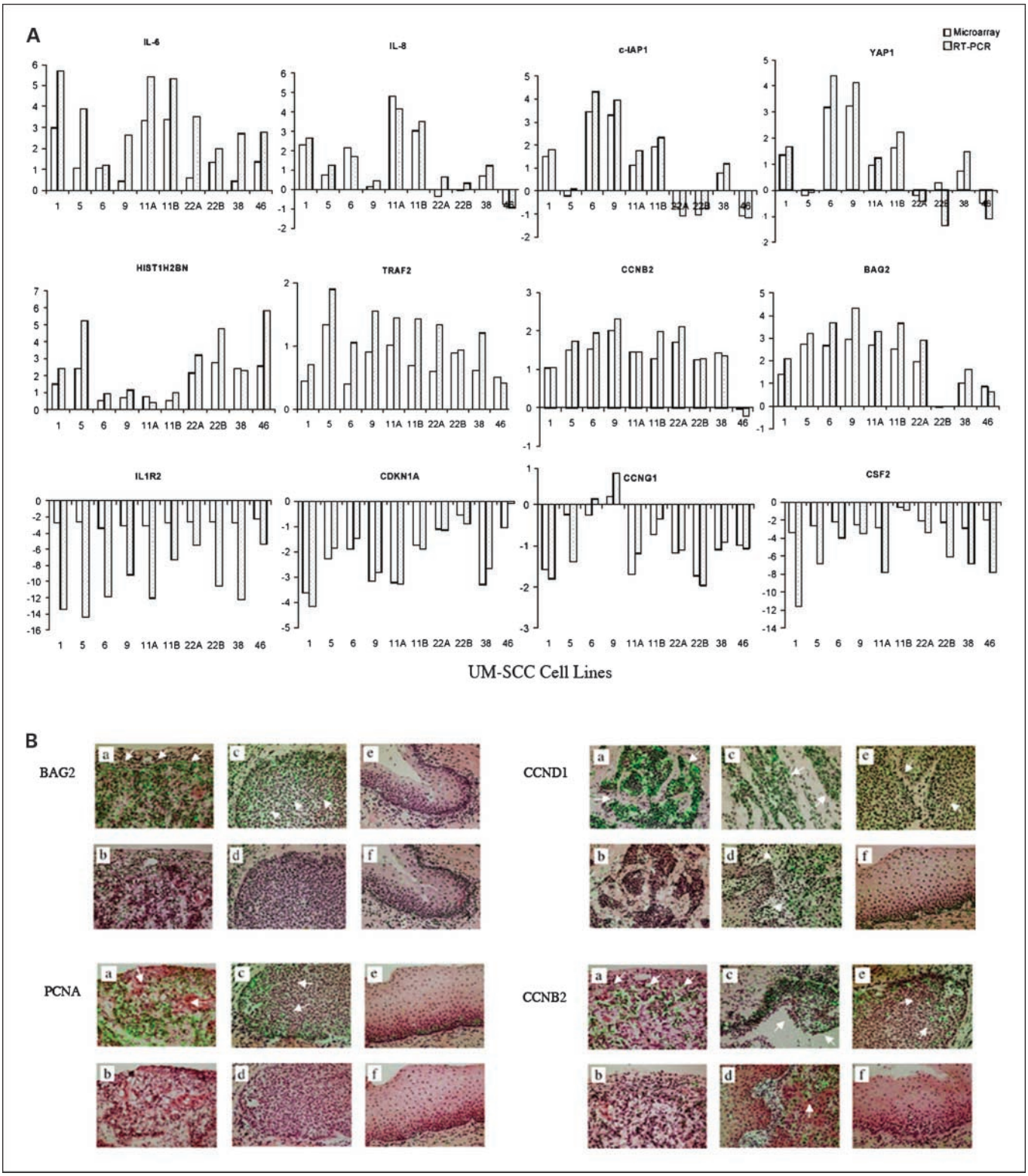

Fig. 2. Validation of microarray data using real-time RT-PCR and *in situ* hybridization. *A,* 12 genes were selected from the microarray experiment, of which 8 were from up-regulated gene group and 4 were from down-regulated gene group. The data are presented as the expression ratio in UM-SCC cell lines to human normal keratinocytes using both data from microarray (*open square*), and real-time RT-PCR (*dotted square*). *B,* detection of *BAG2, PCNA, CCND1*, and *CCNB2* genes in HNSCC tissues and normal mucosa by *in situ* hybridization with the antisense probes specific for each gene (*a*). Sense probes were used as negative controls (*b*). Signals of *in situ* hybridization exhibited as green particles which are indicated by white arrows on the H&E-stained tissues. In each, UM-SCC 11A xenograft tumor section served as the positive control hybridized with antisense probes (*a*) and negative control with sense probes (*b*). For *BAG2* and *PCNA* genes (*left*), HNSCC tumor samples hybridized with antisense probes were in (*c*) or sense probes in (*d*); normal mucosa samples hybridized with antisense probes were in (*e*), or sense probes in (*f*). For *CCND1* and *CCNB2* genes (*right*), the HNSCC tumor samples (*c, e*), the tissues containing both tumor and normal mucosa (*d*), and the normal mucosa (*f*) were hybridized with sense probe. Photomicrographs were taken under 100× magnification.

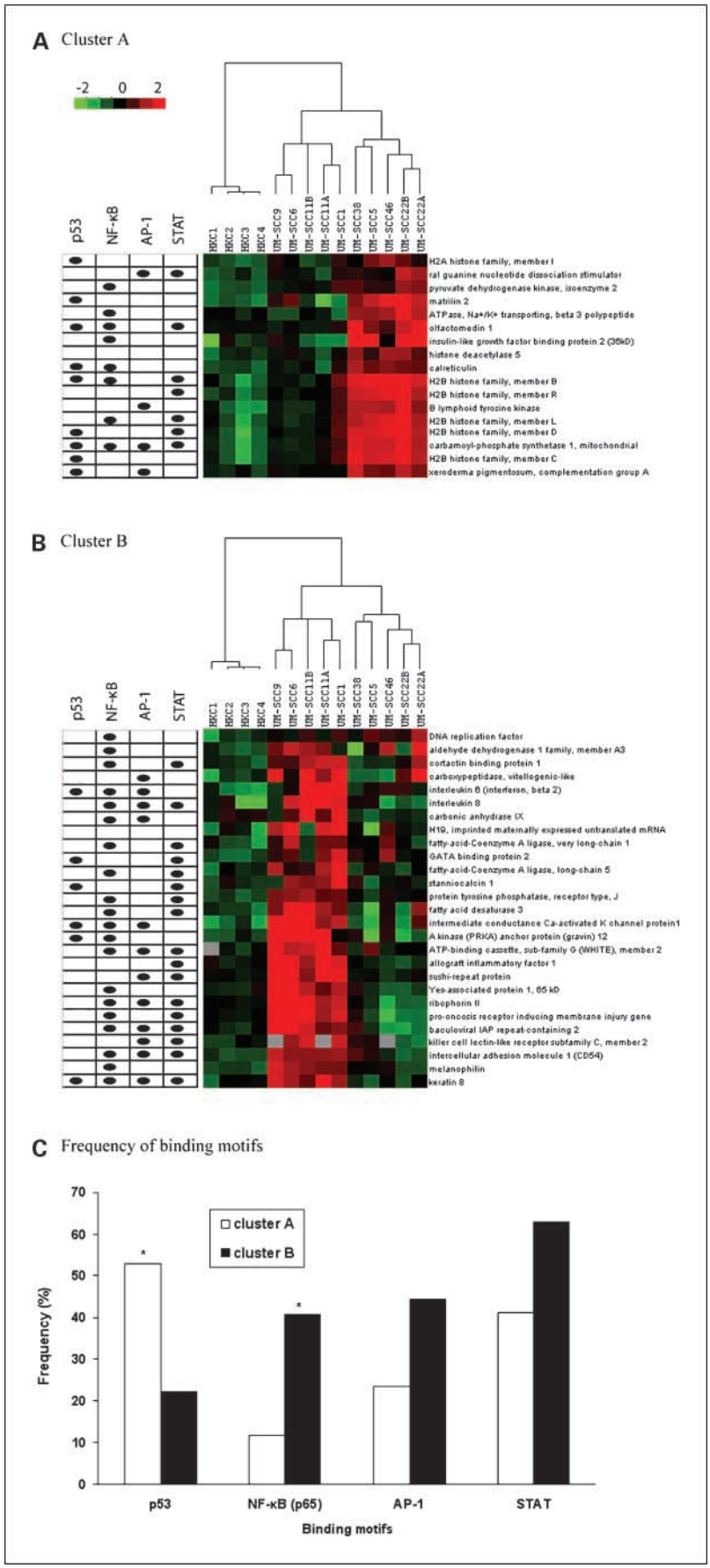

Fig. 3. Identification of transcription factor binding motifs in promoters of the genes in clusters A or B. Differentially expressed genes from clusters A (*A*) and B (*B*) are listed, and the putative transcription factor binding motifs for NF-κB, TP53, AP-1, and STAT were predicted in the proximal gene promoter region by Genomatix Suite. One black dot, one or more predicted binding site on the proximal promoter region (see Supplementary Table S3 for detailed analysis). *C,* the frequency of the predicted binding motifs was calculated in each cluster and analyzed by χ^2 statistical method. A significant difference was observed in TP53 and NF-κB p65 binding motifs between the clusters; *, $P < 0.05$. No statistical significance of AP-1 and STAT predicted frequencies were observed between two clusters of the genes.

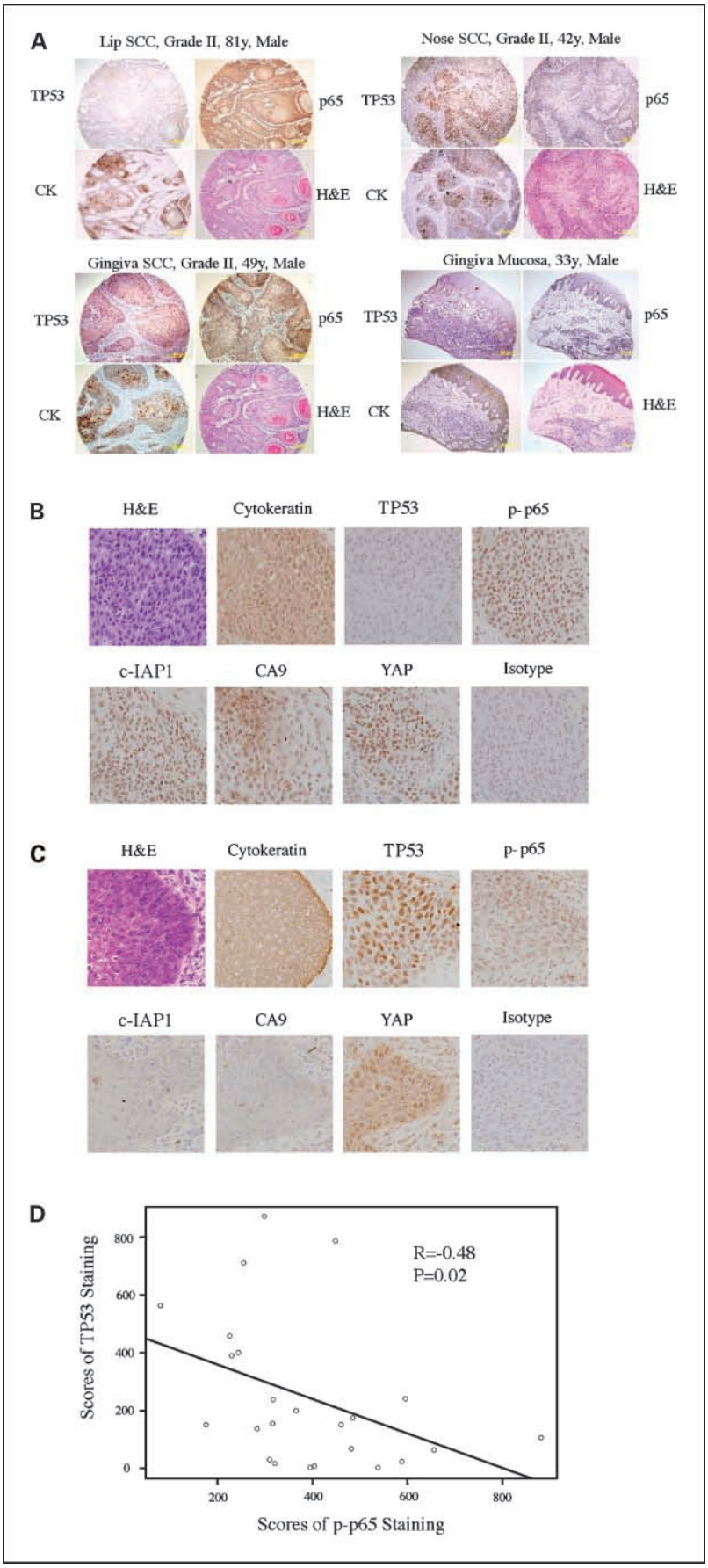

Fig. 4. Immunohistochemistry of TP53, NF-κB, and related protein expression in HNSCC tissues. *A,* immunostaining of TP53 (*top left* in each group), NF-κB p65 (p65, *top right*), and pan-cytokeratin (CK, *bottom left*), as well as H&E staining (*bottom right*) were carried out on tumor and normal mucosa (*bottom right*) samples using human HNSCC tissue array. All photomicrographs were taken under 100× magnification. *B* and *C,* immunohistochemistry of TP53, phospho – NF-κB p65, and its target gene products, CA9, c-IAP1, and YAP were carried on the frozen sections of HNSCC tissues. H&E staining and immunostaining of pan-cytokeratin were used to identify tumor cells from surrounding stroma. The pictures were taken under 400× magnification. *D,* linear regression analysis showed an inverse correlation with statistical significance between increasing TP53 and decreasing phospho – NF-κB p65 staining.

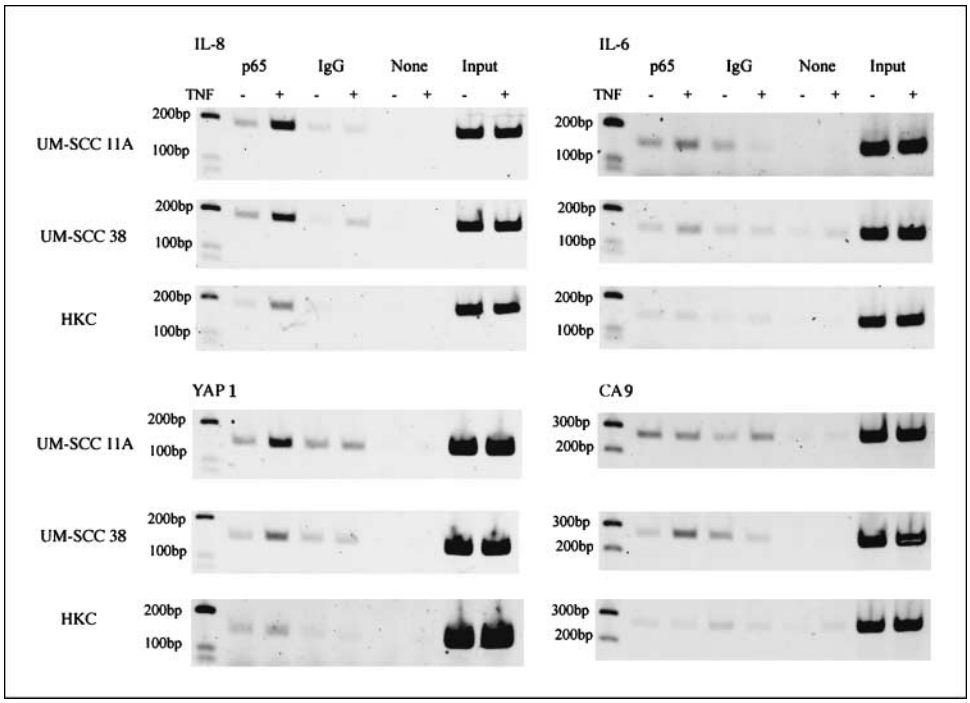

Fig. 5. ChIP assay confirmed the predicted transcription factor binding sites in the promoter regions. *IL-8, IL-6, YAP1*, and *CA9* genes from cluster B were selected with the putative NF-κB binding sites, and ChIP assay was done using rabbit anti-human NF-κB p65 antibody in UM-SCC 11A, 38, and HKC. TNF-α was used as an inducer for NF-κB activity. The same amount of matched isotype antibody was used as the negative control (*IgG*), as well as no antibody controls (*None*). The input DNA was used as the loading control for DNA templates in PCR reaction.

staining for either factor was observed in six normal mucosa controls (*bottom right*). These observations suggested that a portion of HNSCC tumors exhibits a predominant immunostaining by either TP53 or NF-κB p65.

We further explored if a relationship exists between immunostaining for the activated Ser^{536} phosphorylated form of p65 RelA, expression of putative NF-κB regulated cluster B proteins, and TP53 in tumor tissues from patients with HNSCC. To optimally detect undenatured antigens recognized by antibodies to Ser^{536} phosphorylated form of p65 and cluster B proteins, we stained frozen HNSCC tissues from de-identified specimens from a series of 24 patients (including oral cavity, pharynx, and larynx). Again, a subset of HNSCC stained predominantly for either phospho-Ser^{536} NF-κB p65 (Fig. 4B) or TP53 (Fig. 4C). Strong nuclear NF-κB phospho-p65 staining was associated with co-staining for cluster B proteins c-IAP1, YAP, and CA9 (Fig. 4B). In contrast, HNSCC tumors with strong TP53 nuclear staining showed relatively weaker staining of phosphorylated NF-κB p65 and c-IAP1, CA9 proteins from cluster B (Fig. 4C). YAP protein was detected in this set of tumor sections, but with a different staining pattern (more cytoplasmic than nuclear staining; Fig. 4C). To quantify and determine the potential relationship of TP53 and phospho–NF-κB p65, we scored the intensity and percent positivity of the immunostaining and plotted and examined the results by linear regression and statistical analysis. An inverse and statistically significant correlation between increasing nuclear NF-κB phospho-p65 and TP53 staining was observed (Fig. 4D; R = -0.48 and P = 0.02, Spearman rank test).

Detection of predicted NF-κB binding sites in the promoters of cluster B genes by ChIP assay. To obtain evidence whether NF-κB p65 binds to predicted sites in the cluster B gene promoters (Fig. 2 and Supplementary Table S3), chromatin immunoprecipitation (ChIP) assay was done using anti–NF-κB p65 antibody with an isotype immunoglobulin G (IgG) as a negative control (Fig. 5). In Fig. 5, constitutive NF-κB p65 binding to the *IL-8* promoter was observed, and treatment by tumor necrosis factor-α (TNF-α), a known stimulus for NF-κB binding activity, further increased the binding. The induction was greater in UM-SCC 11A cells, and the weakest effect was observed in HKC, consistent with our previous studies of *IL-8* gene activation and expression patterns in these cell lines (19, 20, 23, 41, 44). Similar or weaker constitutive and TNF-inducible binding activities of NF-κB p65 to the *IL-6*, *YAP1*, or *CA9* promoters were observed, with the induction being relatively stronger in UM-SCC 11A cells (Fig. 5). In each case, the binding activity with p65 antibody was greater than the background in negative control lanes using the isotype IgG.

Effects of modulation of NF-κB p65 on cluster B gene expression and cell death. To examine the regulatory role of NF-κB p65 activation on selected cluster B genes and their functional significance in HNSCC with undetectable expression of wt TP53 protein, we examined the effect of knocking down NF-κB p65 by RNAi on modulation of NF-κB transactivation, its downstream gene expression, and cell survival. As shown in Fig. 6A, a significant suppression of NF-κB reporter activity was observed in two wt TP53 cell lines (UM-SCC 1 and 9) transiently transfected with NF-κB p65 RNAi. The expression of three representative genes from each cluster was compared by real-time RT-PCR. Inhibition of NF-κB p65 activity resulted in significant modulation of the expression of cluster B genes *IL-6*, *IL-8*, and *YAP1*, but had no effect on the expression of the genes of cluster A (*HIST1H2BD*, *HIST1H2BN*, and *CALR*), consistent with the regulation of the former genes by NF-κB (Fig. 6B). Although the promoters of *HIST1H2BD* and *CALR* contain putative NF-κB binding motifs (Fig. 2A and Supplementary Table S3), both of them are preferred motifs for p50 but not p65 subunit of NF-κB.[5]

We next tested if knockdown of NF-κB p65 affects growth or the phenotype of HNSCC. Cells were transfected either

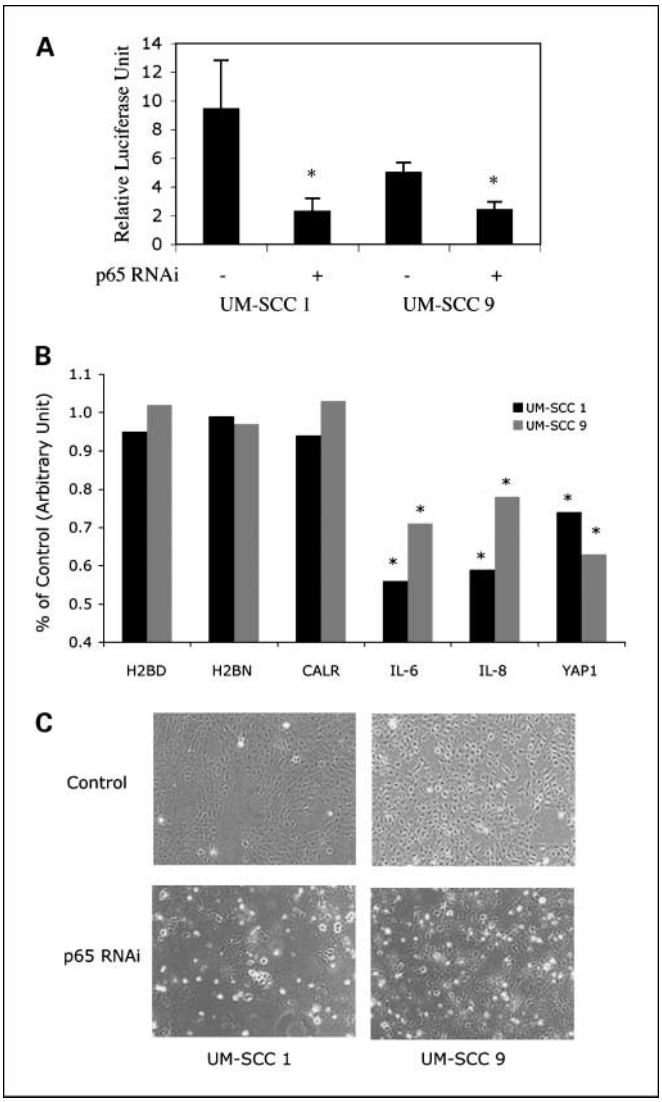

Fig. 6. Modulation of NF-κB altered gene expression and cell survival. *A,* UM-SCC cell lines with wt *TP53* (UM-SCC 1 and 9) were transiently transfected with p65 RNAi oligos or control oligos and 5× NF-κB luciferase and RSV-LacZ plasmids for 48 h, and the reporter activity was measured by luciferase activities. The relative luciferase unit was calculated by normalizing the luciferase to β-gal activities in the same experimental conditions. The experiments were carried out in triplicates, and statistical significance was examined by Student's *t* test; *, $P < 0.05$. *B,* UM-SCC 1 and 9 cells were transiently transfected with a plasmid containing p65 RNAi or control plasmid for 48 h. RNA was isolated, and real-time RT-PCR analysis was done for *IL-6, IL-8*, and *YAP1* from cluster B gene list. The experiments were carried out in triplicates, and statistical significance was examined by Student's *t* test; *, $P < 0.05$. *C,* UM-SCC 1 and 9 cells were transiently transfected with plasmid containing p65 RNAi or control plasmid for 72 h. Cell morphology was captured under an inverted microscope (100×).

with a control or NF-κB p65 RNAi, and morphology was monitored over 72 h. As shown in Fig. 6C, compared with the control-transfected cells, which exhibited a relatively low proportion of rounded and dead cells (*top*), cells transfected by NF-κB p65 RNAi showed increased cell round-up, membrane blebbing, fragmentation, and detachment, all indicative of cell death (*bottom*). Knockdown of NF-κB p65 by RNAi and induction of cell death in UM-SCC lines were confirmed by Western blot, DNA fragmentation, and DNA flow cytometry in independent experiments (19). Together, these data indicated that knocking down NF-κB p65 inhibited the expression of the cluster B genes examined and induced cell death, consistent with our previous data showing that inhibition of NF-κB by overexpression of a dominant negative IκBα or p65 small interfering RNA (siRNA) is associated with decreased cell survival of human or murine SCC (18–20, 22).

Discussion

Previous molecular profiling studies of HNSCC and other cancers have linked distinct gene expression patterns to differences in malignant potential or response to therapy. However, the regulatory and functional relationships underlying different gene expression patterns have not been well defined. In this study, cDNA microarray expression profiling distinguished normal keratinocytes from malignant HNSCC cells and stratified HNSCC further into two subgroups, each exhibiting distinctive gene signatures (Fig. 1). A possible regulatory role of the interactions between NF-κB and TP53 was suggested to underlie the inverse expression of the two discrete gene signatures by bioinformatic analysis of transcription factor binding sites in the promoters of the two gene clusters (Fig. 3). In support of this hypothesis, we confirmed that increased staining for NF-κB p65 and its target gene products was inversely correlated with immunostaining for TP53 in subsets of HNSCC tissue specimens, indicating the relevance of the pattern and relationship observed in HNSCC lines (Fig. 4). NF-κB p65 binding to the promoters of sample genes in cluster B was detected by ChIP assay and was inducible by TNF-α (Fig. 5). We further confirmed that the expression of NF-κB signature genes and cell survival were inhibited by p65 RNAi (Fig. 6; ref. 19). These findings illustrate that bioinformatic analysis of gene promoter regulatory elements and ontology of clustered genes identified by genomic profiling can generate biologically meaningful hypotheses and reveal underlying molecular mechanisms that regulate the differentially expressed genes defining the malignant phenotypes in subsets of HNSCC.

The constitutive activation of NF-κB, inactivation or mutation of *TP53*, and their interaction in affecting the expression of NF-κB and TP53 regulated genes could represent important alternative mechanisms for malignant progression and help explain differences in pathogenicity, resistance to chemoradiotherapy, and poorer prognosis previously associated with the subset of HNSCC with inactivated TP53. With regard to NF-κB, we previously showed that NF-κB is aberrantly activated with malignant progression, modulates the expression of clusters of important oncogenes in murine SCC, and promotes survival, tumorigenesis, and therapeutic resistance of murine and human HNSCCs (18–25, 40, 56–58). Increased activation of NF-κB revealed by clustered coexpression of NF-κB related genes was also recently shown by array profiling in association with malignant progression in SCC arising from skin of α-catenin knock-out mice (59). Zhang et al. (26) confirmed in a clinical study that increased nuclear staining of NF-κB in tissue specimens is associated with the progression of premalignant lesions and decreased prognosis. Chung et al. (60) and Roepman et al. (9) recently identified some of the NF-κB regulated genes among gene signatures expressed by subsets of HNSCC at higher risk for recurrence and metastasis, which were also found in our previous murine (18, 22) and present gene profiling studies.

With regard to TP53 in this study, we recently have found that UM-SCC cells with wt TP53 genotype show lower TP53 RNA and protein expression with defective functionality (33).[6] Hunter et al. recently published a study indicating that inactivation of the p16(INK4a) locus necessary for wt *TP53* expression was associated with isolation of immortalized HNSCC lines and worse prognosis, whereas *TP53* mutation was associated with isolation of mortal HNSCC lines and better prognosis (8). In their study, microarray analysis identified distinct gene expression profiles in the cell lines derived from premalignant squamous dysplasias and HNSCCs in association with these differences in phenotype, *TP53* genotype, and protein expression. Interestingly, a review of their gene list reveals increased expression of some NF-κB regulated genes identified in our previous murine SCC and our present study in cluster B, in the subset associated with the inactivation of *TP53* and greater malignant potential. In another study by Bradford et al. (16, 17), wt *TP53* genotype with low TP53 protein expression has been associated with cisplatin resistance *in vitro* and chemoradiation resistance in patients. This was shown to be inversely related to the expression of BCL-xL (61), another gene which we have shown to be coregulated by NF-κB as well as STAT3 (19).[7] Together, these observations are consistent with our hypothesis that differential expression of NF-κB regulated clustered genes associated with differences in phenotype and clinical outcome is linked to *TP53* status in subsets of HNSCC.

The mechanism(s) underlying this apparent inverse relationship between expression of wt or mutation TP53 protein and NF-κB p65 nuclear localization and target genes in HNSCC cell lines and specimens remains to be determined. This relationship resembles that observed with wt TP53 in previous studies by Perkins (62, 63), who found that deficient expression of wt TP53 protein (*TP53* null) is permissive for the transactivation of NF-κB target genes and cell survival in embryonic fibroblasts and sarcoma cell lines. Conversely, forced expression of wt TP53 protein inhibited transactivation by NF-κB of target genes and cell survival. They found that TP53 protein can compete for CBP/p300, resulting in the increased association of NF-κB with histone deacetylase and repression, with no reduction in NF-κB DNA binding activities (64). Conversely, strong activation of NF-κB was shown to have a reciprocal competing and repressive effect on TP53 stability and transactivation (65). Alternatively, Gurova et al. (66) reported that decreased expression of wt TP53 can result from NF-κB activation through a distinct but unknown mechanism in renal cell carcinoma cell lines. Whether TP53 inactivation or NF-κB activation are primary events and how NF-κB activation and its regulated cluster B gene expression are linked to TP53 in HNSCC is under investigation.

That p65 RNAi suppressed NF-κB reporter activity and the expression of cluster B genes including *IL-6*, *IL-8*, and *YAP1* and induced cell death suggest potential functional relevance of cluster B genes (Fig. 6; ref. 19). These results are consistent with previous reports that link several NF-κB regulated genes identified in cluster B to malignancy, metastasis, resistance to chemoradiotherapy, and/or decreased survival. We previously showed that, in a murine SCC model, murine homologues of cluster B genes *IL-8* (*Gro-1*), *cIAP1* (*cIap-1*), and *YAP1* (*Yap-1*) were coexpressed concomitantly with increased NF-κB activation and tumorigenic and metastatic potential, and they are down-modulated by the inhibition of NF-κB (18, 22, 57). Overexpression of *Gro-1* alone promotes tumorigenesis and metastasis (58). A similar role for *IL-8* has been shown in xenograft models of other human cancers (67). *c-IAP1* is known to be an inhibitor of cell apoptosis and as a target gene regulated by NF-κB and TNF pathways (68). *YAP1* has been reported to promote oncogenic activity, related to the interaction with TP53 family member p73 (69, 70). Both *c-IAP1* and *YAP1* are amplified and contribute to the development of hepatocellular carcinoma in murine models (71). The NF-κB regulated genes *IL-6*, *IL-8*, *GRO-1*, and/or *c-IAP1* have also been detected as potential disease and prognostic markers in studies of tumor, serum, or saliva of HNSCC patients (72–74). *IL-8* was detected by microarray in a subset of tumor samples from a series of 41 patients with recurrent HNSCC (6). Therapeutic resistance to chemotherapy agents paclitaxel and cisplatinum has been independently associated with gene expression of *IL-6* and *IL-8* or *c-IAP1* and *YAP1* (5, 75). We have shown increased *IL-6* and *IL-8* in cell line supernatants and serum from a subset of HNSCC patients and found that these cytokines increase in those resistant to chemoradiation therapy (42, 76). In a phase I clinical study, we observed the inhibition of activated nuclear phospho-p65, *c-IAP1* in tumor, and *IL-6* and *IL-8* in serum in association with increased apoptosis and tumor reduction in a subset of patients given bortezomib, an inhibitor of proteasome-dependent activation of NF-κB (25). Together, these results provide evidence suggesting that cluster B genes are likely associated with NF-κB activation, progression, cell survival, and therapeutic response of SCC.

Less is known about the regulation, significance, and effects of increase in genes identified in the cluster A signature. TP53 binding motifs were present at a higher prevalence in the proximal promoter regions of cluster A genes, where histone H2A and H2B family genes are highly represented (Fig. 2 and Supplementary Table S3). A few other H2A and H2B family genes have been detected in HNSCC cells in prior microarray and proteomics studies (7, 60, 73, 77–79). However, little is known about the biological significance of increased H2A and H2B gene expression or the potential association with TP53 (Fig. 3). Previous studies indicate that repression of histone gene expression occurs with the activation of wt TP53 by UV radiation (80), whereas their expression is increased by the expression of the SV40 T antigen, which inactivates wt TP53 protein (81). It remains to be determined whether overexpression of cluster A genes in this subset of UM-SCC could result from altered TP53 function or activation or interactions with other TP53 family members or cofactors.

Bioinformatics analysis of the promoter binding motifs has been used mostly in the prokaryotic or lower eukaryotic organisms to identify transcriptomes, and limited utilities have been reported following the analysis of global gene expression in human cancers. Using this approach, we identified differences in the prevalence of TP53 or NF-κB binding motifs in the genes of prominent gene clusters. We found evidence for an inverse relationship between expression of these distinct clusters, inactivation or mutation of TP53, and NF-κB activation. A more comprehensive global and computational

[6] Friedman et al., in preparation.
[7] Lee et al., in preparation.

analysis of the gene expression profiles, binding motifs of promoters, and potential pathway networks have been recently carried out in the same set of microarray data from UM-SCC cells and presented elsewhere.[8] Our findings provided evidence that bioinformatic analysis of gene promoter regulatory elements can reveal the critical control mechanisms governing the gene signatures identified from genome-wide gene expression profiling data, which could generate biologically meaningful hypothesis and clinically useful biomarkers to accelerate experimental investigation.

[8] Bin Yan, submitted for publication.

Acknowledgments

We are grateful to Drs. Thomas E. Carey and Carol R. Bradford (University of Michigan, Ann Arbor, MI) for providing UM-SCC cell lines and related clinical data; Dr. Paul S. Albert (Biometric Research Branch, National Cancer Institute/NIH) for his assistance in biostatistical analysis of the immunostaining data; and the Cooperative Human Tissue Network for providing the HNSCC tumor specimens. We express our gratitude to Drs. David Gius (NCI/NIH) and Paul Meltzer (NHGRI/NIH) for their critical reading and helpful comments.

References

1. Choi P, Chen C. Genetic expression profiles and biologic pathway alterations in head and neck squamous cell carcinoma. Cancer 2005;104:1113–28.
2. Jeon GA, Lee JS, Patel V, et al. Global gene expression profiles of human head and neck squamous carcinoma cell lines. Int J Cancer 2004;112:249–58.
3. Warner GC, Reis PP, Makitie AA, et al. Current applications of microarrays in head and neck cancer research. Laryngoscope 2004;114:241–8.
4. Gonzalez HE, Gujrati M, Frederick M, et al. Identification of 9 genes differentially expressed in head and neck squamous cell carcinoma. Arch Otolaryngol Head Neck Surg 2003;129:754–9.
5. Akervall J, Guo X, Qian CN, et al. Genetic and expression profiles of squamous cell carcinoma of the head and neck correlate with cisplatin sensitivity and resistance in cell lines and patients. Clin Cancer Res 2004; 10:8204–13.
6. Ginos MA, Page GP, Michalowicz BS, et al. Identification of a gene expression signature associated with recurrent disease in squamous cell carcinoma of the head and neck. Cancer Res 2004;64:55–63.
7. Chung CH, Parker JS, Karaca G, et al. Molecular classification of head and neck squamous cell carcinomas using patterns of gene expression. Cancer Cell 2004; 5:489–500.
8. Hunter KD, Thurlow JK, Fleming J, et al. Divergent routes to oral cancer. Cancer Res 2006;66:7405–13.
9. Roepman P, Kemmeren P, Wessels LF, Slootweg PJ, Holstege FC. Multiple robust signatures for detecting lymph node metastasis in head and neck cancer. Cancer Res 2006;66:2361–6.
10. Gonzalez MV, Pello MF, Lopez-Larrea C, Suarez C, Menendez MJ, Coto E. Loss of heterozygosity and mutation analysis of the p16 (9p21) and p53 (17p13) genes in squamous cell carcinoma of the head and neck. Clin Cancer Res 1995;1:1043–9.
11. Kropveld A, van Mansfeld AD, Nabben N, Hordijk GJ, Slootweg PJ. Discordance of p53 status in matched primary tumours and metastases in head and neck squamous cell carcinoma patients. Eur J Cancer B Oral Oncol 1996;32B:388–93.
12. van Houten VM, Snijders PJ, van den Brekel MW, et al. Biological evidence that human papillomaviruses are etiologically involved in a subgroup of head and neck squamous cell carcinomas. Int J Cancer 2001; 93:232–5.
13. Braakhuis BJ, Snijders PJ, Keune WJ, et al. Genetic patterns in head and neck cancers that contain or lack transcriptionally active human papillomavirus. J Natl Cancer Inst 2004;96:998–1006.
14. Clayman GL, el-Naggar AK, Lippman SM, et al. Adenovirus-mediated p53 gene transfer in patients with advanced recurrent head and neck squamous cell carcinoma. J Clin Oncol 1998;16:2221–32.
15. Vogelstein B, Kinzler KW. Cancer genes and the pathways they control. Nat Med 2004;10:789–99.
16. Bradford CR, Zhu S, Ogawa H, et al. P53 mutation correlates with cisplatin sensitivity in head and neck squamous cell carcinoma lines. Head Neck 2003;25: 654–61.
17. Bradford CR, Zhu S, Wolf GT, et al. Overexpression of p53 predicts organ preservation using induction chemotherapy and radiation in patients with advanced laryngeal cancer. Department of Veterans Affairs Laryngeal Cancer Study Group. Otolaryngol Head Neck Surg 1995;113:408–12.
18. Dong G, Loukinova E, Chen Z, et al. Molecular profiling of transformed and metastatic murine squamous carcinoma cells by differential display and cDNA microarray reveals altered expression of multiple genes related to growth, apoptosis, angiogenesis, and the NF-κB signal pathway. Cancer Res 2001;61: 4797–808.
19. Duan J, Friedman J, Nottingham L, Chen Z, Ara G, Van Waes C. Nuclear factor-KB p65 small interfering RNA or proteasome inhibitor bortezomib sensitizes head and neck squamous cell carcinomas to classic histone deacetylase inhibitors and novel histone deacetylase inhibitor PXD101. Mol Cancer Ther 2007; 6:37–50.
20. Duffey DC, Chen Z, Dong G, et al. Expression of a dominant-negative mutant inhibitor-κBα of nuclear factor-κB in human head and neck squamous cell carcinoma inhibits survival, proinflammatory cytokine expression, and tumor growth *in vivo*. Cancer Res 1999;59:3468–74.
21. Kato T, Duffey DC, Ondrey FG, et al. Cisplatin and radiation sensitivity in human head and neck squamous carcinomas are independently modulated by glutathione and transcription factor NF-κB. Head Neck 2000;22:748–59.
22. Loercher A, Lee TL, Ricker JL, et al. Nuclear factor-κB is an important modulator of the altered gene expression profile and malignant phenotype in squamous cell carcinoma. Cancer Res 2004;64:6511–23.
23. Ondrey FG, Dong G, Sunwoo J, et al. Constitutive activation of transcription factors NF-(κ)B, AP-1, and NF-IL6 in human head and neck squamous cell carcinoma cell lines that express pro-inflammatory and pro-angiogenic cytokines. Mol Carcinog 1999;26: 119–29.
24. Duffey DC, Crowl-Bancroft CV, Chen Z, et al. Inhibition of transcription factor nuclear factor-κB by a mutant inhibitor-κBα attenuates resistance of human head and neck squamous cell carcinomas to TNF-α caspase-mediated cell death. Br J Cancer 2000;83: 1367–74.
25. Van Waes C, Chang AA, Lebowitz PF, et al. Inhibition of nuclear factor-κB and target genes during combined therapy with proteasome inhibitor bortezomib and reirradiation in patients with recurrent head-and-neck squamous cell carcinoma. Int J Radiat Oncol Biol Phys 2005;63:1400–12.
26. Zhang PL, Pellitteri PK, Law A, et al. Overexpression of phosphorylated nuclear factor-κ B in tonsillar squamous cell carcinoma and high-grade dysplasia is associated with poor prognosis. Mod Pathol 2005;18: 924–32.
27. Barnes PJ, Karin M. Nuclear factor-κB: a pivotal transcription factor in chronic inflammatory diseases. N Engl J Med 1997;336:1066–71.
28. Blackwell TS, Christman JW. The role of nuclear factor-κB in cytokine gene regulation. Am J Respir Cell Mol Biol 1997;17:3–9.
29. Karin M, Delhase M. The IκB kinase (IKK) and NF-κB: key elements of proinflammatory signalling. Semin Immunol 2000;12:85–98.
30. Pahl HL. Activators and target genes of Rel/NF-κB transcription factors. Oncogene 1999;18:6853–66.
31. Richmond A. NF-κB, chemokine gene transcription and tumour growth. Nat Rev Immunol 2002;2:664–74.
32. Schmidt-Ullrich R, Memet S, Lilienbaum A, Feuillard J, Raphael M, Israel A. NF-κB activity in transgenic mice: developmental regulation and tissue specificity. Development 1996;122:2117–28.
33. Yan B, Yang X, Lee TL, Friedman J, Tang J, Van Waes C, Chen Z. Genome-wide identification of novel expression signatures reveal distinct patterns and prevalance of binding motifs for p53, nuclear factor-κB and other signal transcription factors in head and neck squamous cell carcinoma. Genome Biol 2007;8:R78.
34. Chen Z, Lee TL, Yang XP, Dong G, Loercher A, Van Waes C. cDNA microarray and bioinformatic analysis of nuclear factor-κB related genes in squamous cell carcinoma. In: Fisher PD, editor. Cancer genomics and proteomics: methods and protocols. Totowa (NJ): Humana Press; 2007. In press.
35. Chen Y, Dougherty ER, Bittner ML. Ratio-based decisions and the quantitative analysis of cDNA microarray images. J Biomed Opt 1997;2:364–74.
36. Eisen MB, Spellman PT, Brown PO, Botstein D. Cluster analysis and display of genome-wide expression patterns. Proc Natl Acad Sci U S A 1998;95: 14863–8.
37. Saldanha AJ. Java Treeview-extensible visualization of microarray data. Bioinformatics 2004;20:3246–8.
38. Wolfinger RD, Gibson G, Wolfinger ED, et al. Assessing gene significance from cDNA microarray expression data via mixed models. J Comput Biol 2001;8:625–37.
39. Tempelman RJ. Assessing statistical precision, power, and robustness of alternative experimental designs for two color microarray platforms based on mixed effects models. Vet Immunol Immunopathol 2005;105:175–86.
40. Bancroft CC, Chen Z, Yeh J, et al. Effects of pharmacologic antagonists of epidermal growth factor receptor, PI3K and MEK signal kinases on NF-κB and AP-1 activation and IL-8 and VEGF expression in human head and neck squamous cell carcinoma lines. Int J Cancer 2002;99:538–48.
41. Chen Z, Colon I, Ortiz N, et al. Effects of interleukin-1α, interleukin-1 receptor antagonist, and neutralizing antibody on proinflammatory cytokine expression by human squamous cell carcinoma lines. Cancer Res 1998;58:3668–76.
42. Chen Z, Malhotra PS, Thomas GR, et al. Expression of proinflammatory and proangiogenic cytokines in patients with head and neck cancer. Clin Cancer Res 1999;5:1369–79.
43. Lee TL, Yeh J, Van Waes C, Chen Z. Epigenetic modification of SOCS-1 differentially regulates STAT3 activation in response to interleukin-6 receptor and epidermal growth factor receptor signaling through

JAK and/or MEK in head and neck squamous cell carcinomas. Mol Cancer Ther 2006;5:8–19.
44. Wolf JS, Chen Z, Dong G, et al. IL (interleukin)-1α promotes nuclear factor-κB and AP-1–induced IL-8 expression, cell survival, and proliferation in head and neck squamous cell carcinomas. Clin Cancer Res 2001;7:1812–20.
45. Li Y, Elashoff D, Oh M, et al. Serum circulating human mRNA profiling and its utility for oral cancer detection. J Clin Oncol 2006;24:1754–60.
46. Li Y, St John MA, Zhou X, et al. Salivary transcriptome diagnostics for oral cancer detection. Clin Cancer Res 2004;10:8442–50.
47. Yang P, Sun Z, Aubry MC, et al. Study design considerations in clinical outcome research of lung cancer using microarray analysis. Lung Cancer 2004;46:215–26.
48. Wei C, Li J, Bumgarner RE. Sample size for detecting differentially expressed genes in microarray experiments. BMC genomics 2004;5:87.
49. Boyle JO, Hakim J, Koch W, et al. The incidence of p53 mutations increases with progression of head and neck cancer. Cancer Res 1993;53:4477–80.
50. Koch WM, Brennan JA, Zahurak M, et al. p53 mutation and locoregional treatment failure in head and neck squamous cell carcinoma. J Natl Cancer Inst 1996;88:1580–6.
51. Freier K, Joos S, Flechtenmacher C, et al. Tissue microarray analysis reveals site-specific prevalence of oncogene amplifications in head and neck squamous cell carcinoma. Cancer Res 2003;63:1179–82.
52. Rocha S, Martin AM, Meek DW, Perkins ND. p53 represses cyclin D1 transcription through down regulation of Bcl-3 and inducing increased association of the p52 NF-κB subunit with histone deacetylase 1. Mol Cell Biol 2003;23:4713–27.
53. Amin MA, Haas CS, Zhu K, et al. Migration inhibitory factor up-regulates vascular cell adhesion molecule-1 and intercellular adhesion molecule-1 via Src, PI3 kinase, and NFκB. Blood 2006;107:2252–61.
54. Aoudjit F, Brochu N, Belanger B, Stratowa C, Hiscott J, Audette M. Regulation of intercellular adhesion molecule-1 gene by tumor necrosis factor-α is mediated by the nuclear factor-κB heterodimers p65/p65 and p65/c-Rel in the absence of p50. Cell Growth Differ 1997;8:335–42.
55. Jahnke A, Johnson JP. Synergistic activation of intercellular adhesion molecule 1 (ICAM-1) by TNF-α and IFN-γ is mediated by p65/p50 and p65/c-Rel and interferon-responsive factor Stat1 α (p91) that can be activated by both IFN-γ and IFN-α. FEBS Lett 1994;354:220–6.
56. Dong G, Chen Z, Kato T, Van Waes C. The host environment promotes the constitutive activation of nuclear factor-κB and proinflammatory cytokine expression during metastatic tumor progression of murine squamous cell carcinoma. Cancer Res 1999;59:3495–504.
57. Loukinova E, Chen Z, Van Waes C, Dong G. Expression of proangiogenic chemokine Gro 1 in low and high metastatic variants of Pam murine squamous cell carcinoma is differentially regulated by IL-1α, EGF and TGF-β1 through NF-κB dependent and independent mechanisms. Int J Cancer 2001;94:637–44.
58. Loukinova E, Dong G, Enamorado-Ayalya I, et al. Growth regulated oncogene-α expression by murine squamous cell carcinoma promotes tumor growth, metastasis, leukocyte infiltration and angiogenesis by a host CXC receptor-2 dependent mechanism. Oncogene 2000;19:3477–86.
59. Kobielak A, Fuchs E. Links between α-catenin, NF-κB, and squamous cell carcinoma in skin. Proc Natl Acad Sci U S A 2006;103:2322–7.
60. Chung CH, Parker JS, Ely K, et al. Gene expression profiles identify epithelial-to-mesenchymal transition and activation of nuclear factor-{κ}B signaling as characteristics of a high-risk head and neck squamous cell carcinoma. Cancer Res 2006;66:8210–8.
61. Bauer JA, Trask DK, Kumar B, et al. Reversal of cisplatin resistance with a BH3 mimetic, (-)-gossypol, in head and neck cancer cells: role of wild-type p53 and Bcl-xL. Mol Cancer Ther 2005;4:1096–104.
62. Rocha S, Garrett MD, Campbell KJ, Schumm K, Perkins ND. Regulation of NF-κB and p53 through activation of ATR and Chk1 by the ARF tumour suppressor. EMBO J 2005;24:1157–69.
63. Webster GA, Perkins ND. Transcriptional cross talk between NF-κB and p53. Mol Cell Biol 1999;19:3485–95.
64. Rocha S, Campbell KJ, Perkins ND. p53- and Mdm2-independent repression of NF-κB transactivation by the ARF tumor suppressor. Mol Cell 2003;12:15–25.
65. Tergaonkar V, Pando M, Vafa O, Wahl G, Verma I. p53 stabilization is decreased upon NFκB activation: a role for NFκB in acquisition of resistance to chemotherapy. Cancer Cell 2002;1:493–503.
66. Gurova KV, Hill JE, Guo C, et al. Small molecules that reactivate p53 in renal cell carcinoma reveal a NF-κB–dependent mechanism of p53 suppression in tumors. Proc Natl Acad Sci U S A 2005;102:17448–53.
67. Arenberg DA, Kunkei SL, Polverini PJ, Burdick MD, Strieter RM. Inhibition of interleukin-8 reduces tumorigenesis of human non-small cell lung cancer in SCID mice. J Clin Invest 1996;97:2792–802.
68. Wang CY, Mayo MW, Korneluk RG, Goeddel DV, Baldwin AS, Jr. NF-κB antiapoptosis: induction of TRAF1 and TRAF2 and c-IAP1 and c-IAP2 to suppress caspase-8 activation. Science 1998;281:1680–3.
69. Basu S, Totty NF, Irwin MS, Sudol M, Downward J. Akt phosphorylates the Yes-associated protein, YAP, to induce interaction with 14-3-3 and attenuation of p73-mediated apoptosis. Mol Cell 2003;11:11–23.
70. Overholtzer M, Zhang J, Smolen GA, et al. Transforming properties of YAP, a candidate oncogene on the chromosome 11q22 amplicon. Proc Natl Acad Sci U S A 2006;103:12405–10.
71. Zender L, Spector MS, Xue W, et al. Identification and validation of oncogenes in liver cancer using an integrative oncogenomic approach. Cell 2006;125:1253–67.
72. Alevizos I, Mahadevappa M, Zhang X, et al. Oral cancer *in vivo* gene expression profiling assisted by laser capture microdissection and microarray analysis. Oncogene 2001;20:6196–204.
73. Jarvinen AK, Autio R, Haapa-Paananen S, et al. Identification of target genes in laryngeal squamous cell carcinoma by high-resolution copy number and gene expression microarray analyses. Oncogene 2006;25:6997–7008.
74. Li HM, Zhuang ZH, Wang Q, et al. Epstein-Barr virus latent membrane protein 1 (LMP1) upregulates Id1 expression in nasopharyngeal epithelial cells. Oncogene 2004;23:4488–94.
75. Duan Z, Feller AJ, Penson RT, Chubner BA, Seiden MV. Discovery of differentially expressed genes associated with paclitaxel resistance using cDNA array technology: analysis of IL-6, IL-8, and monocyte chemotatic protein 1 in the paclitaxel-resistant phenotype. Clin Cancer Res 1999;5:3445–53.
76. Druzgal CH, Chen Z, Yeh NT, et al. A pilot study of longitudinal serum t (cytokine) and angiogenesis factor levels as markers of therapeutic response and survival in patients with head and neck squamous cell carcinoma. Head Neck 2005;27:771–84.
77. Baker H, Patel V, Molinolo AA, et al. Proteome-wide analysis of head and neck squamous cell carcinomas using laser-capture microdissection and tandem mass spectrometry. Oral Oncol 2005;41:183–99.
78. Carles A, Millon R, Cromer A, et al. Head and neck squamous cell carcinoma transcriptome analysis by comprehensive validated differential display. Oncogene 2006;25:1821–31.
79. Sriuranpong V, Mutirangura A, Gillespie JW, et al. Global gene expression profile of nasopharyngeal carcinoma by laser capture microdissection and complementary DNA microarrays. Clin Cancer Res 2004;10:4944–58.
80. Su C, Gao G, Schneider S, et al. DNA damage induces downregulation of histone gene expression through the G1 checkpoint pathway. EMBO J 2004;23:1133–43.
81. Wolff J, Wong C, Cheng H, Poyet P, Butel JS, Rosen JM. Differential effects of the simian virus 40 early genes on mammary epithelial cell growth, morphology, and gene expression. Exp Cell Res 1992;202:67–76.